

INFLUENCE OF DIFFUSION OF ATOMS ON THE DARK RESONANCE LINESHAPE IN SPATIALLY BOUNDED LASER FIELDS

V.I. ROMANENKO and L.P. YATSENKO

*Institute of Physics, Nat. Acad. of Sci. of Ukraine and
46, Nauky Ave., Kyiv 03680, Ukraine**

A.V. ROMANENKO

*Taras Shevchenko National University of Kyiv and
2, Academician Glushkov Ave., Kyiv 03022, Ukraine*

Abstract

We propose a diffusion model for the recently discovered diffusion-induced Ramsey narrowing arising when atoms diffuse in a buffer-gas cell in the laser radiation field. The diffusion equation for the coherence of metastable states coupled with an excited state by laser radiation of different frequencies in a three-level scheme of the atom-field interaction is obtained in the strong-collision approximation. The dependence of the shape of an absorption line near the transmission maximum of one of the frequencies on the two-photon resonance detuning for various geometries of the cell is investigated.

PACS numbers: 42.50.Gy, 42.50.Hz, 32.80.Qk, 33.80.Be

*Electronic address: vr@iop.kiev.ua

I. INTRODUCTION

In a three-level system subjected to two laser fields coupling two metastable states (or a metastable state and a stable one) with an excited one, a dark or light-nonabsorbing state, namely a coherent superposition of two metastable states, can be formed. This phenomenon is called a coherent population trapping (CPT). The condition of the formation of a CPT state is the two-photon resonance under interaction of an atom with light, where the difference between the frequencies of two laser fields is equal to the frequency of a transition between metastable states. If this condition is realized, one observes an abrupt decrease of the fluorescence intensity of the atom in the laser radiation field [1–3]. Due to the CPT phenomenon, it is possible to create a window in the absorption spectrum. As a result, light can propagate almost without losses through a medium that absorbs light under usual conditions, which represents the well-known phenomenon of electromagnetically induced transparency (EIT) [4]. In addition, dark resonances are used for the light slowing down [5] and in the construction of compact laser frequency standards [6] and underlie the effective method of population transfer between different states of atoms or molecules – stimulated Raman adiabatic passage (STIRAP) [7]. The resonance width depends on both the coherence decrease rate for the lower states and on other factors, particularly on the pattern of atomic motion in a buffer-gas cell. The latter aspect will be the focus of our attention in this work.

In the case where atoms move through a laser beam of finite width, the role of the coherence time is played by the residence time of an atom in the field. If the cell contains a buffer gas in addition to active atoms, their residence time in the laser beam increases. As a result, narrow resonances with a width of the order of tens of hertzs are registered in buffer-gas cells [9]. The authors of works [8–10] emphasize the role of the buffer gas in the experiments on coherent population trapping in a three-level system, though it is considered that, after atoms have left the region of interaction with radiation, they do not return there anymore.

A more detailed description of the process of atom-field interaction must take into account that, having left the region of interaction with the field, the atom can return there again [11, 12], so that atoms can interact with radiation several times before the loss of coherence. Thus, diffusion of atoms in a buffer gas essentially affects their response to the resonance

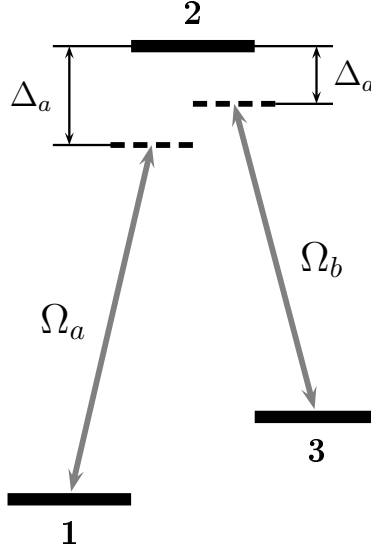


FIG. 1: Three-level system: Ω_a and Ω_b are the Rabi frequencies

excitation by the laser field. If the coherence relaxation time of the metastable states considerably exceeds the time till the repeated atom-field interaction, the atom can get back without loss of coherence after having spent some time in a dark region (beyond the beam). As a result, it is worth expecting the narrowing of the resonance line. This phenomenon was called a diffusion-induced Ramsey narrowing [13] (by analogy with the Ramsey method of separated oscillating fields [14, 15]).

The diffusion-induced Ramsey narrowing of the transmission spectrum in the case of EIT observations was investigated in [13] adducing the results of experiments with rubidium vapor and neon serving as a buffer gas, as well as the results of theoretical calculations. According to [13], the necessity of taking the diffusion process into account depends on the laser-beam diameter – the contribution made into the signal by atoms that had spent some time beyond the beam and got back becomes determinative with decrease in the beam diameter. The same authors subsequently published a detailed description of the developed theory [16]. Experimental results and theoretical calculations unambiguously confirm the physical interpretation of the phenomenon of diffusion-induced Ramsey narrowing of the transmission spectrum observed in [13]. In particular, with increase in the laser-beam diameter or the buffer gas pressure, the shape of the spectral line changes from the non-Lorentz to Lorentz one in accordance with a decrease of the contribution made by atoms that have come back from the region beyond the laser field. In the cited works, the motion of atoms is

described in the form of the Ramsey sequences: in each of them, an atom spends the time t_1^{in} in the radiation field, moves in the dark region during the time t_2^{out} , returns back to the radiation region for the time t_3^{in} , and so on. In order to find the transmission spectrum, the density matrix describing the Ramsey sequence was integrated with the probability distribution, i.e. one performed averaging over all possible trajectories. The probability distribution was obtained in [16] from the diffusion equation.

We propose an alternative approach to the description of the diffusion-induced Ramsey narrowing. It is based on the diffusion equation obtained from the initial motion equations for the density matrix on the basis of the strong-collision approximation [8, 17]. The transmission spectrum will be directly obtained in the equilibrium approach instead of averaging over trajectories. As compared to works [13] and [16], we consider the relaxation at cell walls (supposing that the coherence is broken due to a collision of an atom with the wall) and take a realistic (Gaussian) intensity distribution in the radial direction. In addition, we also take the finiteness of the gas cell in the direction parallel to the laser beam into account. In order to understand how the dimension of the problem influences the result, we also consider the one-dimensional case where the cell is infinite in the direction of the laser beam, while the beam itself is infinite along one of the transverse coordinates.

II. BASIC EQUATIONS

Let us consider a gas of three-level atoms with the excited state $|2\rangle$ and the metastable lower states $|1\rangle$ and $|3\rangle$. A field with the frequency ω_a couples the states $|1\rangle$ and $|2\rangle$, while that with the frequency ω_b couples the states $|3\rangle$ and $|2\rangle$ (see Fig. 1). The interaction of these fields with atoms is described by the Rabi frequencies $\Omega_a = \boldsymbol{\mu}_{12} \cdot \mathbf{E}_a / \hbar$ and $\Omega_b = \boldsymbol{\mu}_{32} \cdot \mathbf{E}_b / \hbar$, respectively. As the beams a and b are spatially bounded, the Rabi frequencies depend on the position \mathbf{r} of an atom in space. The wave vectors will be considered close in magnitude: $k_a \simeq k_b \simeq k$.

The equations for nondiagonal elements of the density matrix in the rotating-wave approximation have the form

$$\dot{\rho}_{12} = i(\Delta_a - kv)\rho_{12} + \frac{i\Omega_a^*}{2}(\rho_{22} - \rho_{11}) -$$

$$-\frac{i\Omega_b^*}{2}\rho_{13} + \left(\frac{\partial\rho_{12}}{\partial t}\right)_{\text{relax}} + \left(\frac{\partial\rho_{12}}{\partial t}\right)_{\text{coll}}, \quad (1)$$

$$\dot{\rho}_{23} = -i(\Delta_b - kv)\rho_{23} + \frac{i\Omega_a}{2}\rho_{13} + \frac{i\Omega_b}{2}(\rho_{33} - \rho_{22}) + \left(\frac{\partial\rho_{23}}{\partial t}\right)_{\text{relax}} + \left(\frac{\partial\rho_{23}}{\partial t}\right)_{\text{coll}}, \quad (2)$$

$$\dot{\rho}_{31} = -i(\Delta_a - \Delta_b)\rho_{31} - \frac{i\Omega_a}{2}\rho_{23}^* + \frac{i\Omega_b^*}{2}\rho_{12}^* + \left(\frac{\partial\rho_{31}}{\partial t}\right)_{\text{relax}} + \left(\frac{\partial\rho_{31}}{\partial t}\right)_{\text{coll}}. \quad (3)$$

Here, the terms with the index “coll” describe the relaxation processes due to collisions of active atoms (interacting with the field) with atoms of the buffer gas resulting in a change of the velocity, while the coherence is conserved. The terms with the index “relax” describe the rest of relaxation processes, $\Delta_a = \omega_{21} - \omega_a$ and $\Delta_b = \omega_{23} - \omega_b$ are the one-photon detunings, and $\Delta\omega = \Delta_a - \Delta_b$ is the two-photon detuning. It is assumed that

$$\left(\frac{\partial\rho_{12}}{\partial t}\right)_{\text{relax}} = -\Gamma_{12}\rho_{12}, \quad \left(\frac{\partial\rho_{23}}{\partial t}\right)_{\text{relax}} = -\Gamma_{23}\rho_{23},$$

where Γ_{12} and Γ_{23} stand for the coherence relaxation rates for the transitions $2 \rightarrow 1$ and $2 \rightarrow 3$, respectively. If Γ_{13} and Γ_{23} are sufficiently large, the collision terms in Eqs. (1) and (2) can be neglected. The relaxation rate for the forbidden transition $|1\rangle \rightarrow |3\rangle$ is non-zero due to collisions between atoms,

$$\left(\frac{\partial\rho_{31}}{\partial t}\right)_{\text{relax}} = -\gamma_{13}\rho_{31}. \quad (4)$$

In the general case, the expression for the collision term [18–20] can be presented as

$$\begin{aligned} \left(\frac{\partial\rho_{ij}(\mathbf{v}, \mathbf{v}', t)}{\partial t}\right)_{\text{coll}} &= -\nu\rho_{ij}(\mathbf{v}, \mathbf{v}', t) + \\ &+ \int K_{ij}(\mathbf{v}', \mathbf{v})\rho_{ij}(\mathbf{r}, \mathbf{v}', t) d\mathbf{v}', \end{aligned} \quad (5)$$

where $K_{ij}(\mathbf{v}', \mathbf{v})$ is the collision kernel, and ν is, in the general case, a complex-valued quantity with the frequency dimension. It can be interpreted as the collision frequency in the case where the scattering amplitudes in both states i and j are identical (see [18]).

The collision term can be simplified using the strong-collision approximation (light atoms are scattered by heavy particles [17]) and assuming that ν and K_{ij} are real, while the kernel $K_{ij}(\mathbf{v}', \mathbf{v})$ does not depend on \mathbf{v}' , i.e. the velocity of an atom \mathbf{v} after a collision does not depend on its velocity \mathbf{v}' before it. In this case, the velocity distribution (arbitrary in the general case) turns into the Maxwellian distribution after only several collisions, that is, an atom quickly forgets its initial velocity. As was shown in [17], $K_{ij}(\mathbf{v}) = \nu W(\mathbf{v})$, where $W(\mathbf{v})$ is the Maxwellian distribution. Thus [20], expression (5) takes the form

$$\left(\frac{\partial \rho_{ij}}{\partial t} \right)_{\text{coll}} = -\nu [\rho_{ij} - W(\mathbf{v}) N_{ij}],$$

$$\text{where } N_{ij}(\mathbf{r}, t) = \int d\mathbf{v} \rho_{ij}(\mathbf{r}, \mathbf{v}, t) \quad (6)$$

can be interpreted as the number of atoms with values of ρ_{ij} lying in the unit volume in the neighborhood of the point \mathbf{r} , and ν denotes the collision frequency [18].

In this approximation, collisions with the buffer gas change only the external degrees of freedom of atoms.

Using the approximation $|\frac{d}{dt}| \ll \Gamma_{12}, \Gamma_{23}$ and neglecting the collision terms in (1) and (2), one can find the stationary solutions for ρ_{12} and ρ_{23} . After that, with regard for the fact that the nondiagonal elements ρ_{ii} are close to the equilibrium values $\rho_{ii}^{(0)}$ (they differ from the latter by a small quantity of the second order in the field intensity), one obtains the equation for ρ_{31} :

$$\begin{aligned} \dot{\rho}_{31} = & -(\gamma_{13} + i\Delta\omega)\rho_{31} - \\ & - \left[\frac{\Omega_a^* \Omega_a}{\Gamma_{23} - i(\Delta_b - kv)} + \frac{\Omega_b^* \Omega_b}{\Gamma_{12} + i(\Delta_a - kv)} \right] \rho_{31} \\ & - \frac{\Omega_a \Omega_b^*}{4} \left[\frac{\rho_{11}^{(0)} - \rho_{22}^{(0)}}{\Gamma_{12} + i(\Delta_a - kv)} + \frac{\rho_{33}^{(0)} - \rho_{22}^{(0)}}{\Gamma_{23} - i(\Delta_b - kv)} \right] + \\ & + \left(\frac{\partial \rho_{31}}{\partial t} \right)_{\text{coll}}. \end{aligned} \quad (7)$$

The second term on the right-hand side describes the field broadening. It can be neglected in the case of weak fields and large relaxation rates Γ_{ij} .

In order to simplify the equation, we also neglect the Doppler broadening in the third term considering that $\Gamma_{ij} \gg \Delta_{a,b}, \Delta\omega, kv$.

Taking into account that the equilibrium elements of the density matrix ρ_{ii} are proportional to the distribution function $W(\mathbf{v})$, we obtain a kinetic equation of the Boltzmann type for ρ_{31} .

In the stationary case of interest, it has the following form:

$$\begin{aligned} (\mathbf{v} \cdot \nabla) \rho(\mathbf{r}, \mathbf{v}) = & -(\nu + \gamma + i\Delta\omega) \rho(\mathbf{r}, \mathbf{v}) \\ & + W(\mathbf{v}) [\lambda(\mathbf{r}) + \nu N(\mathbf{r})]. \end{aligned} \quad (8)$$

Here and below, we use the notations

$$\begin{aligned} \rho(\mathbf{r}, \mathbf{v}) &= \rho_{31}(\mathbf{r}, \mathbf{v}), \quad \gamma = \gamma_{13}, \\ N &= N_{31}, \quad W(\mathbf{v}) = W_0 e^{-\mathbf{v}^2/v_0^2}, \end{aligned}$$

where N_{31} is determined by (6), and W_0 is the normalization constant of the Maxwellian distribution,

$$\lambda(\mathbf{r}) = \frac{1}{4} \left(\frac{\rho_{11}^{(0)}}{\Gamma_{12}} + \frac{\rho_{33}^{(0)}}{\Gamma_{13}} \right) \Omega_a \Omega_b^*. \quad (9)$$

Here, we took into account that $\rho_{22}^{(0)} \ll \rho_{11}^{(0)}$, $\rho_{22}^{(0)} \ll \rho_{33}^{(0)}$. As one can see from (9), the function $\lambda(\mathbf{r}) \sim \Omega_a(\mathbf{r})\Omega_b^*(\mathbf{r})$ describes the transverse profile of the beams.

For the sake of simplicity, we introduce the substitution

$$\alpha_0 = \gamma + i\Delta\omega, \quad \alpha = \nu + \gamma + i\Delta\omega = \nu + \alpha_0.$$

It is assumed that the collisions of atoms with walls result in the failure of the coherence between the lower states, so that

$$\rho(\mathbf{r}, \mathbf{v})|_{\mathbf{r} \in S} = 0,$$

where S denotes the surface confining the buffer-gas cell.

The shape of the spectral line is determined by the function $T(\Delta\omega) = \text{Re} [S(\Delta\omega)/S(0)]$, where $S(\Delta\omega)$ has the form

$$S(\Delta\omega) = \iint d\mathbf{r} d\mathbf{v} \lambda(\mathbf{r}) \rho(\mathbf{r}, \mathbf{v}) = \int \lambda(\mathbf{r}) N(\mathbf{r}) d\mathbf{r}. \quad (10)$$

In order to find it, it is necessary to obtain the function ρ .

In the case of a laser beam with the Gaussian intensity distribution in the plane normal to the direction of its propagation, the expression for $\lambda(\mathbf{r})$ in the cylindrical coordinates takes the form

$$\lambda(r, \varphi, z) = \lambda_0 e^{-r^2/a^2}, \quad (11)$$

where λ_0 is determined by (9), and \mathbf{r} lies at the beam axis.

In the strong-collision approximation, the time between collisions $\tau_\nu = 1/\nu$ is small as compared to the characteristic time of flight of an atom through the interaction region $\tau_a = a/v_0$. Therefore, we consider that $\nu\tau_a \gg 1$.

In what follows, we investigate the effect of the beam size and the distance to the walls of the gas cell on the lineshape specified by the function $\text{Re } S(\Delta\omega)$. The form of this function depending on the dimension of the problem will be considered as well.

III. SOLUTION FOR INFINITE REGION

For an infinite region, Eq. (8) can be solved with the help of the Fourier transformation with respect to the argument \mathbf{r} :

$$\hat{\rho}(\mathbf{k}, \mathbf{v}) = \int \rho(\mathbf{r}, \mathbf{v}) e^{-i\mathbf{k}\cdot\mathbf{r}} d\mathbf{r}, \quad \hat{N}(\mathbf{k}) = \int \hat{\rho}(\mathbf{k}, \mathbf{v}) d\mathbf{v}.$$

Hence,

$$\hat{N}(\mathbf{k}) = \frac{\hat{\lambda}(\mathbf{k}) \hat{F}(\mathbf{k})}{1 - \nu \hat{F}(\mathbf{k})}, \quad (12)$$

where the function

$$\hat{F}(\mathbf{k}) = \int \frac{W(\mathbf{v}) d\mathbf{v}}{\alpha + i\mathbf{k}\mathbf{v}} = \frac{\sqrt{\pi}}{|k|v_0} e^{\alpha^2/k^2v_0^2} \text{erfc}\left(\frac{\alpha}{|k|v_0}\right),$$

describes the Voigt profile. Let us find the signal S_∞ using the properties of the Fourier transformation:

$$S_\infty(\Delta\omega) = \int d\mathbf{r} N(\mathbf{r}) \lambda(\mathbf{r}) = \frac{1}{(2\pi)^n} \int d\mathbf{k} \hat{N}(\mathbf{k}) \hat{\lambda}(\mathbf{k}), \quad (13)$$

where n denotes the space dimension of the region (1, 2, or 3). Substituting N from (12), we obtain

$$S_\infty(\Delta\omega) = \frac{1}{(2\pi)^n} \int \frac{\hat{\lambda}^2(\mathbf{k}) \hat{F}(\mathbf{k})}{1 - \nu \hat{F}(\mathbf{k})} d\mathbf{k}.$$

In some cases, the value of $S(\Delta\omega)$ is mainly determined by small k due to the factor $\hat{\lambda}^2(k)$. That is why the function $\hat{F}(k)$ can be replaced by the asymptotic expansion in the quadratic approximation (see [21]):

$$S_\infty(\Delta\omega) \simeq \frac{1}{(2\pi)^n} \int \frac{\hat{\lambda}^2(\mathbf{k}) d\mathbf{k}}{\alpha_0 + \frac{k^2 v_0^2}{2\alpha}}. \quad (14)$$

It is valid for sufficiently small k , for which $|k|v_0/\nu \ll 1$.

A. One-dimensional case

In the given case, $\lambda(x) = \lambda_0 e^{-x^2/a^2}$, and (14) has the form

$$\begin{aligned} S_\infty^{(1)}(\Delta\omega) &= \frac{\lambda_0^2 a}{2} \int_{-\infty}^{\infty} \frac{e^{-u^2/2}}{\alpha_0 + u^2/\tau_D} du = \\ &= \frac{\pi \lambda_0^2 a^3}{2} \frac{\beta}{\alpha_0} e^{\beta^2 a^2/2} \operatorname{erfc}\left(\frac{\beta a}{\sqrt{2}}\right), \end{aligned} \quad (15)$$

where

$$\beta^2 = \frac{2\alpha\alpha_0}{v_0^2}, \quad \tau_D = \frac{2\alpha a^2}{v_0^2}, \quad \beta^2 a^2 = \tau_D \alpha_0$$

(the quantity τ_D will be interpreted below). In our approximation, $\nu \gg \gamma, \Delta\omega$, that is why one can consider $\tau_D = \text{const}$. The right-hand side of (15) can be presented in the form of a superposition of the profiles

$$S_\infty^{(1)}(\Delta\omega) \sim \int_{-\infty}^{\infty} s(\Delta\omega, u) g_\infty^{(1)}(u) du, \quad (16)$$

where

$$s(\Delta\omega, u) = \frac{\gamma_{\text{eff}}(u)}{\gamma_{\text{eff}}(u) + i\Delta\omega}, \quad \gamma_{\text{eff}}(u) = \gamma + u^2/\tau_D$$

with the weighting factor (independent of ω)

$$g_\infty^{(1)}(u) = \frac{1}{\gamma_{\text{eff}}(u)} e^{-u^2/2}. \quad (17)$$

The combination $\tau(u) = \tau_D/u^2$ can be called the effective diffusion time of an atom; $\tau(u)$ for “fast” atoms is larger than that for “slow” ones.

The profile $S_\infty^{(1)}(\Delta\omega)$ can be described as the effective Lorentzian with the center at the origin of coordinates

$$S_L(\Delta\omega) = \frac{\Gamma_0}{\Gamma_0 + i\Delta\omega}.$$

Its width Γ_0 is determined by the relation

$$\Gamma_0^2 = -\frac{2S(0)}{S''(0)}.$$

Simple calculations for $\gamma\tau_D \ll 1$ yield

$$\Gamma_0^2 = \frac{8}{3}\gamma^2 \cdot \left(1 - \sqrt{\frac{2}{\pi}} \sqrt{\gamma\tau_D} + \dots\right). \quad (18)$$

Therefore, we obtain $\Gamma_0 \simeq \sqrt{\frac{8}{3}}\gamma$ for small γ .

B. Two-dimensional case

Using the similar procedure for the function $\lambda(\mathbf{r}) = \lambda_0 e^{-r^2/a^2}$ in the polar coordinates, we obtain

$$\begin{aligned} S_\infty^{(2)}(\Delta\omega) &= \frac{\pi\lambda_0^2 a^2}{2} \int_0^\infty \frac{u e^{-u^2/2} du}{\alpha_0 + u^2/\tau_D} = \\ &= \frac{\pi\lambda_0^2 a^4}{4\alpha_0} e^{\beta^2 a^2/2} \text{Ei}_1\left(\frac{\beta^2 a^2}{2}\right). \end{aligned} \quad (19)$$

Here, Ei_1 denotes the integral first-order exponent[23]. The obtained expression is similar to (15) and has the same interpretation, though with the weighting function

$$g_\infty^{(2)}(u) = \frac{1}{\gamma_{\text{eff}}(u)} u e^{-u^2/2}. \quad (20)$$

The width of the effective Lorentzian for $\gamma\tau_D \ll 1$ has the form

$$\Gamma_0^2 = \gamma^2 2 [\ln 2 - \gamma_E - \ln(\gamma\tau_D)] + o(\gamma\tau_D). \quad (21)$$

IV. EFFECTIVE DIFFUSION EQUATION

A. Derivation of diffusion equation

According to (10), the complex signal $S(\Delta\omega)$ can be expressed with the help of the zero-order momentum $N(\mathbf{r})$ of the distribution $\rho(\mathbf{r})$ with respect to \mathbf{v} . Let us find the equation for the moments of higher orders $N^{(k)}(\mathbf{r})$.

First, we consider the one-dimensional case. Here,

$$N^{(k)}(x) = \int_{-\infty}^{\infty} v^k \rho(x, v) dv, \quad N^{(0)}(x) = N(x).$$

Equation (8) presented in the one-dimensional case as

$$v \frac{\partial \rho(x, v)}{\partial x} = -\alpha \rho(x, v) + W(v) [\lambda(x) + \nu N^{(0)}(x)] \quad (22)$$

will be multiplied by v^k and integrated over v . This procedure yields a chain of equations for the moments $N^{(k)}(x)$.

Writing down the obtained equations separately for even and odd k and successively substituting the following equation into the previous one m times, we obtain the following expression for $N^{(0)}$:

$$\begin{aligned} \alpha N^{(0)} &= \sum_{k=0}^m \frac{\langle v^{2k} \rangle}{\alpha^{2k}} \frac{d^{2k}}{dx^{2k}} [\lambda(x) + \nu N^{(0)}(x)] + \\ &+ \frac{1}{\alpha^{2m+1}} \frac{d^{2m+2} N^{(2m+2)}}{dx^{2m+2}}. \end{aligned} \quad (23)$$

The result for higher space dimensions will be similar, though more complicated as the moments will be specified by tensors. A similar procedure yields

$$\begin{aligned} \alpha N^{(0)}(\mathbf{r}) &= \sum_{k=0}^m \frac{\langle v_{i_1} \dots v_{i_{2k}} \rangle}{\alpha^{2k}} \times \\ &\times (\nabla_{i_1} \dots \nabla_{i_{2k}}) [\lambda(\mathbf{r}) + \nu N^{(0)}(\mathbf{r})] + \dots \end{aligned} \quad (24)$$

Expressions (23) and (24) represent asymptotic expansions, where one can leave only the first terms in the case of sufficiently large ν (and α). In particular, the second-order terms result in the diffusion equation.

Using the known expressions for the averages $\langle v_i v_j \rangle$, one obtains

$$N^{(0)} = \left(1 + \frac{\langle v^2 \rangle}{n\alpha^2} \Delta \right) (\lambda + \nu N^{(0)}) + \dots$$

in the quadratic approximation, where n stands for the space dimension. In view of the equality $\langle v^2 \rangle = \frac{n}{2} v_0^2$, one derives

$$\alpha_0 N(\mathbf{r}) = \frac{\nu v_0^2}{2\alpha^2} \Delta N(\mathbf{r}) + \lambda(\mathbf{r}), \quad N(\infty) = 0 \quad (25)$$

for the arbitrary n (accurate to terms of the order of $1/\nu$). This equation can be interpreted as the diffusion equation with the absorption coefficient $\alpha_0 = \gamma + i\Delta\omega$ and the complex-valued diffusion coefficient

$$\tilde{D} = \frac{\nu v_0^2}{2\alpha^2}. \quad (26)$$

The diffusion coefficient is identical for all space dimensions.

Expression (26) at large ν becomes real and turns into

$$D = \frac{v_0^2}{2\nu}. \quad (27)$$

Proceeding from the formula $a = \sqrt{D\tau_D}$, we obtain the characteristic diffusion time (approximate time, for which an atom leaves the beam)

$$\tau_D = \frac{a^2}{D} = \frac{2a^2\nu}{v_0^2}. \quad (28)$$

For the further consideration, it is convenient to put down the diffusion equation (25) in the form

$$\Delta N(\mathbf{r}) - \beta^2 N(\mathbf{r}) = -f(\mathbf{r}), \quad (29)$$

where $f(\mathbf{r}) = \frac{\beta^2}{\alpha_0} \lambda(\mathbf{r})$, $\beta^2 = \frac{2\alpha_0\alpha^2}{\nu v_0^2} \simeq \frac{\alpha_0\tau_D}{a^2}$. Solving it with the help of the Green function method, one can see that the expression for the signal obtained by solving (29) in the case of large ν will be the same as that obtained earlier by direct calculations (14). One can also see that the number of terms used in the asymptotic expansion $\hat{F}(\mathbf{k})$ of expression (14) correlates with the number of terms of Eq. (24) that must be kept in order to obtain the diffusion equation.

In the case of a finite cell, the kinetic equation (8) can be solved formally, by interpreting the last term on the right-hand side as a nonuniform one (see [22]). The result will be the same as that derived from the solution of (25) accurate to the terms ν^{-2} (to which the diffusion equation is actually valid).

The atomic motion is characterized by five characteristic times:

$$\begin{aligned} \tau_a &= \frac{a}{v_0}, \quad \tau_R = \frac{R}{v_0}, \quad \tau_\gamma = \frac{1}{\gamma}, \\ \tau_\nu &= \frac{1}{\nu}, \quad \tau_D = \frac{a^2}{D} = \nu\tau_a^2. \end{aligned} \quad (30)$$

According to the accepted approximations, they satisfy the following conditions:

$$\tau_\nu < \tau_a < \tau_R, \quad \tau_D < \tau_\gamma, \quad \tau_\nu \ll \tau_\gamma, \quad \tau_a < \tau_D. \quad (31)$$

The first condition results from the strong-collision approximation and the geometric configuration $R > a$ for small ν and (or) large R . The approximation used for the derivation of the diffusion equation will be valid for a finite-size cell. The second and third conditions correspond to the slowness of relaxation processes, while the last condition is evident.

Let us introduce the dimensionless time and space scales $\hat{t} = \gamma t$ and $\hat{r} = r/a$ and denote the dimensionless velocity by $\hat{v}_0 = v_0/(\gamma a)$, the diffusion coefficient by $\hat{D} = D/(\gamma a^2)$, the collision frequency by $\hat{\nu} = \nu/\gamma$, and the cell size by $\hat{R} = R/a$. The dimensionless characteristic times will have the form

$$\begin{aligned} \hat{\tau}_\gamma &= 1, \quad \hat{\tau}_\nu = \gamma \tau_\nu = \frac{1}{\hat{\nu}}, \quad \hat{\tau}_D = \gamma \tau_D = \frac{2\hat{\nu}}{\hat{v}_0^2}, \\ \hat{\tau}_a &= \gamma \tau_a = \frac{1}{\hat{v}_0}, \quad \hat{\tau}_R = \gamma \tau_R = \frac{\hat{R}}{\hat{v}_0}. \end{aligned} \quad (32)$$

As will be seen from the further solution, the shape of the transmission line in the infinite case is completely determined by two dimensionless characteristic times $\hat{\tau}_\nu$ and $\hat{\tau}_D$, whereas, in the case of a finite cell, it depends on its size – \hat{R} (width) and \hat{l} (length, in the three-dimensional case).

The diffusion equation in the form (29) will be solved for different space dimensions. The most effective approach is that based on the Green functions. In order to simplify the comparison of the cases of finite R and $R \rightarrow \infty$, we present the result of investigating the effect of space confinements on the signal in the form most similar to the solution for an infinite cell.

B. One-dimensional case

Using the general solution of the one-dimensional diffusion equation with the boundary conditions $N(\pm R) = 0$, we obtain

$$S_R^{(1)}(\Delta\omega) = \frac{1}{2\pi a} \int_{-\infty}^{+\infty} \frac{\hat{\lambda}(u/a) \hat{\lambda}_R(u/a) du}{\alpha_0 + u^2/\tau_D}, \quad (33)$$

where $\hat{\lambda}_R(u/a) = \hat{\lambda}(u/R)b^{(1)}(u, R)$, and $b^{(1)}(u, R)$ is a factor depending on R :

$$b^{(1)}(u, R) = B^{(1)}(u/a, R),$$

$$B^{(1)}(k, R) = \frac{1}{\hat{\lambda}(k)} \int_{-R}^R \lambda(x) \left[e^{-ikx} - e^{-ikR} \frac{\text{ch}(\beta x)}{\text{ch}(\beta R)} \right] dx. \quad (34)$$

This expression means that, similar to the infinite case (16), $S_R^{(1)}$ can be written down as a superposition of Lorentzians:

$$S_R^{(1)}(\Delta\omega) \sim \int_{-\infty}^{+\infty} s(\Delta\omega, u) g_R^{(1)}(u, \Delta\omega) du,$$

though, in contrast to (17), the weighting function in the case of finite R depends on R and $\Delta\omega$:

$$g_R^{(1)}(u, \Delta\omega) = g_{\infty}^{(1)}(u) b^{(1)}(u, \Delta\omega, R);$$

moreover, $\lim_{R \rightarrow \infty} g_R^{(1)}(u, \Delta\omega) = g_{\infty}^{(1)}(u)$. In the case of $R \rightarrow \infty$, the dependence on $\Delta\omega$ disappears. The factor $g_R^{(1)}(u, \Delta\omega)$ cannot be interpreted as a weighing one due to the dependence on $\Delta\omega$. In addition, the Lorentzian $s(\Delta\omega, u)$ cannot be replaced by the more complicated profile $s_R(\Delta\omega, u) = s(\Delta\omega, u) \cdot b^{(1)}(u, \Delta\omega, R)$ in order to separate out the weight, as it was done in the infinite case, because this “profile” s_R becomes singular for some values of u (in particular, for $u \rightarrow \infty$), though this singularity is compensated by the other factor $g_{\infty}^{(1)}(u)$. Thus, the interpretation of $S_R^{(1)}(\Delta\omega)$ as a weighted superposition is impossible here.

For the Gaussian intensity distribution, the function $b^{(1)}(k, R)$ can be expressed in terms of the error functions:

$$B^{(1,g)}(k, R) = 1 - \frac{\text{erfc}\left(\frac{R}{a} + i\frac{ka}{2}\right) + \text{erfc}\left(\frac{R}{a} - i\frac{ka}{2}\right)}{2} - e^{(k^2 + \beta^2)/4} \frac{\cos kR}{\text{ch}\beta R} \frac{\text{erf}\left(\frac{R}{a} + \frac{\beta a}{2}\right) + \text{erf}\left(\frac{R}{a} - \frac{\beta a}{2}\right)}{2}. \quad (35)$$

In the case $R \gg a$, $\frac{R}{a} \gg \frac{\beta a}{2}$, one can obtain the asymptotic behavior of $B^{(1)}(k, R)$ for small k :

$$B^{(1,g)}(k, R) \simeq 1 - e^{(k^2 + \beta^2)a^2/4} \frac{\cos kR}{\text{ch}\beta R}. \quad (36)$$

The graphs of $\text{Re } S_R(\Delta\omega)$ and the associated parameters for the typical values

$$\gamma = 1.0 \times 10^2 \text{ Hz}, \quad \nu = 1.0 \times 10^6 \text{ Hz},$$

$$a = 1.0 \times 10^{-3} \text{ m}, \quad v_0 = 2.95 \times 10^2 \text{ m/s},$$

and $\tau_D = 2.3 \times 10^{-5} \text{ s}$ with the corresponding dimensionless values

$$\hat{\tau}_D = 2.3 \times 10^{-3}, \quad \hat{\tau}_\nu = 1.0 \times 10^{-4}$$

are given in Fig. 2.

One can see that the line will be narrower for larger R (where the probability to return without loss of coherence is higher). Formally, the geometric factor $g_R^{(1)}(u, \Delta\omega)$ for finite R is larger than $g_\infty^{(1)}(u)$. Therefore, the profile $\text{Re } S_R(\Delta\omega)$ will be wider.

C. Two-dimensional case

Using the axially symmetric solution of the two-dimensional diffusion equation in the region $r < R$ with the boundary condition $N(\mathbf{r})|_{r=R} = 0$, one obtains

$$S_R^{(2)}(\Delta\omega) = \frac{1}{2\pi} \int_0^\infty \frac{u \hat{\lambda}(u/a) \hat{\lambda}_R(u/a) du}{\alpha_0 + u^2/\tau_D} b^{(2)}(u, R), \quad (37)$$

where $\hat{\lambda}_R(u/a) = \hat{\lambda}(u/a) b^{(2)}(u, R)$ and

$$b^{(2)}(u, R) = B^{(2)}(u/a, R),$$

$$B^{(2)}(k, R) = \frac{2\pi}{\hat{\lambda}(k)} \int_0^R r \lambda(r) \left[J_0(kr) - J_0(kR) \frac{I_0(\beta r)}{I_0(\beta R)} \right] dr; \quad (38)$$

moreover, $\lim_{R \rightarrow \infty} b_R^{(2)}(u, R) = 1$.

The same way as in the one-dimensional case, the weighting factor of the Lorentzian has the form $g_R^{(2)}(u, \Delta\omega) = g_\infty^{(2)}(u) b^{(2)}(u, R, \Delta\omega)$. The interpretation of (38) and the comparison with the infinite case (19) are the same as those in the one-dimensional one (35). The graphs of $\text{Re } S_R^{(2)}(\Delta\omega)$ in Fig. 3 are plotted for the same values of the parameters as in Fig. 2.

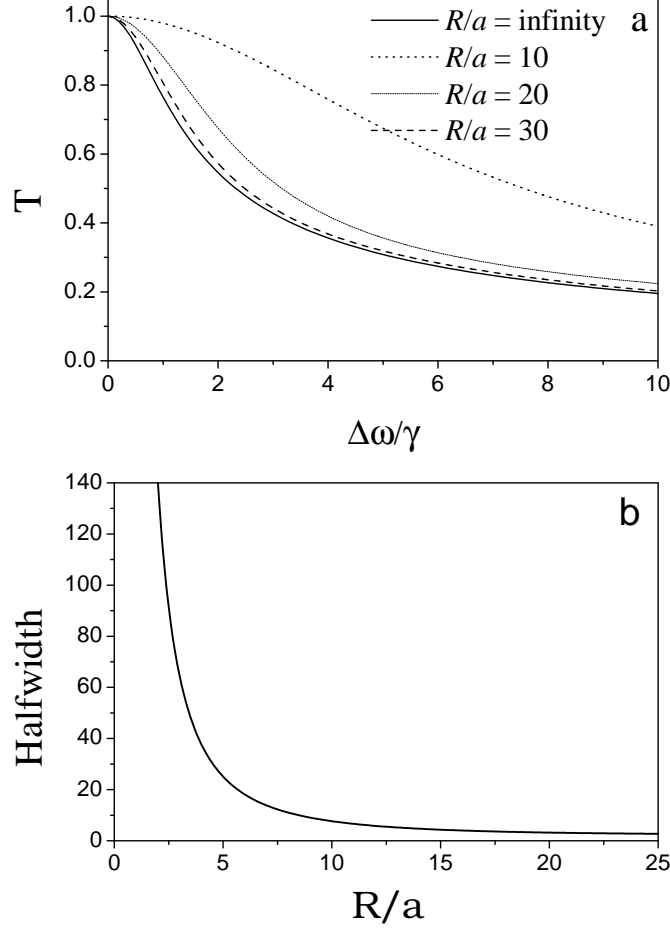


FIG. 2: One-dimensional case: normalized transmission $T = \text{Re} S(\Delta\omega)/S(0)$ as a function of $\Delta\omega/\gamma$ for different R (a) and the transmission spectrum halfwidth as a function of R/a (b). The values of the parameters are given in text

D. Three-dimensional case

In the three-dimensional case where $N(\mathbf{r})$ is zero on the cylindrical surface of radius $r = R$ confined by the planes $z = \pm l$, the diffusion equation is identical to that obtained in the two-dimensional case, whereas the signal has the following form (modified two-dimensional profile):

$$S_R^{(3)}(\Delta\omega) = \frac{l}{16\pi a^2} \frac{\beta^2}{\alpha_0} \times \int_0^\infty du \frac{u \hat{\lambda}^2(u/a)}{\alpha_0 + u^2/\tau_D} b^{(2)}(u, R) b^{(3)}(u, l), \quad (39)$$

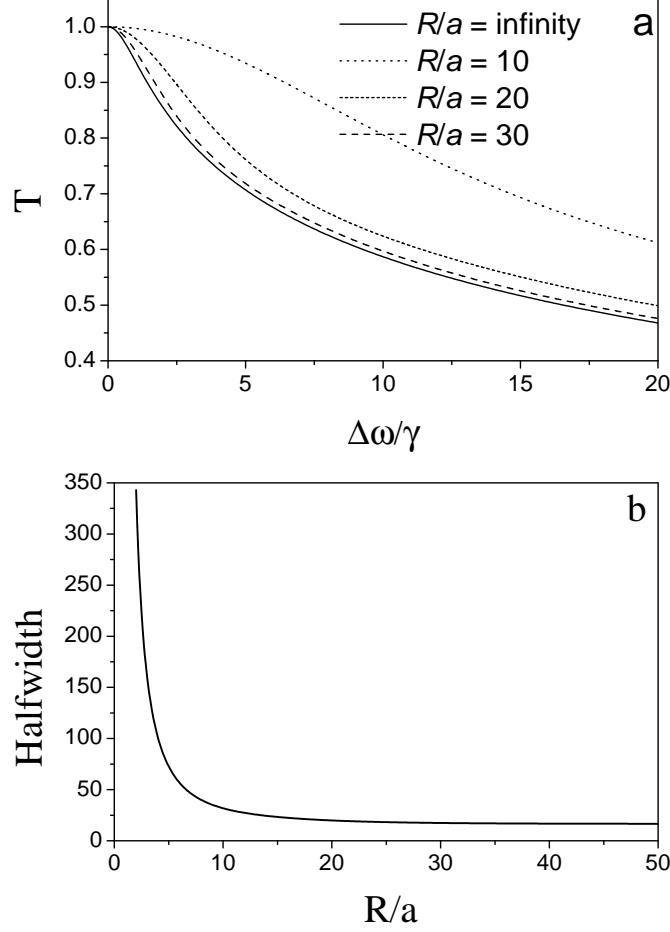


FIG. 3: Two-dimensional case: normalized transmission $T = \text{Re } S_R(\Delta\omega)/S_R(0)$ as a function of $\Delta\omega/\gamma$ for $R = \infty$ and finite R (a) and the transmission spectrum halfwidth as a function of R/a (b). The values of the parameters are the same as in Fig. 2

where $\hat{\lambda}(k)$ denotes the two-dimensional Fourier transform of $\lambda(\mathbf{r})$, $b^{(2)}(u, R)$ is the factor from the two-dimensional case depending on R (see (38)), and

$$b^{(3)}(u, l, \Delta\omega) = 1 - \frac{\tanh \xi(u, \Delta\omega)}{\xi(u, \Delta\omega)},$$

$$\xi(u, \Delta\omega) = \frac{l}{a} \sqrt{u^2 + \beta^2 a^2}. \quad (40)$$

The weighting factor of the Lorentzians in the three-dimensional case (39) has the form

$$\begin{aligned} g_{R,l}^{(3)}(u, \Delta\omega) &= g_R^{(2)}(u) b^{(3)}(u, l) = \\ &= g_\infty^{(2)}(u) b^{(2)}(u, R, \Delta\omega) b^{(3)}(u, l, \Delta\omega). \end{aligned}$$

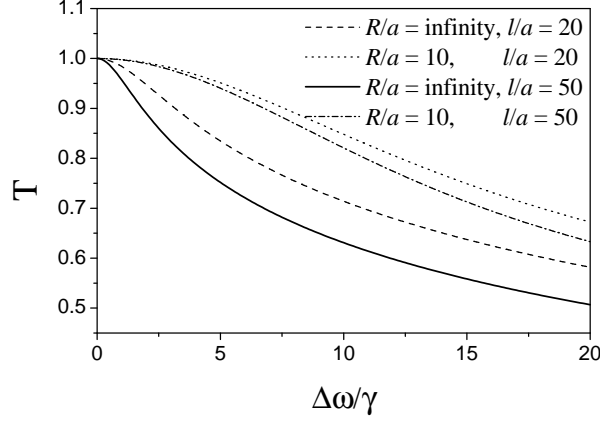


FIG. 4: Three-dimensional case. $T = \text{Re } S_R^{(3)}(\Delta\omega)/S_R^{(3)}(0)$ as a function of $\Delta\omega/\gamma$ for different space parameters

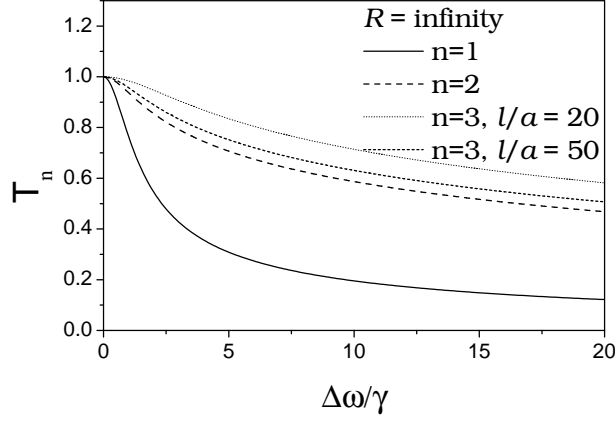


FIG. 5: Comparison of the functions $T_n = \text{Re } S_\infty^{(n)}(\Delta\omega)/S_\infty^{(n)}(0)$ for $n = 1, 2, 3$

Its properties are similar to those in the one- and two-dimensional cases. It is worth noting that its dependence on the cell dimensions R and l appears in the form of independent factors.

The transmission spectra normalized to one at the maximum for different values of the space parameters are given in Fig. 4. As expected, a decrease of l results in the broadening of the spectrum. Figures 5 and 6 present the transmission spectra for all dimensions in the case of an infinite cell and a cell with the size $R/a = 10$. One can see that the narrowest spectrum is obtained in the one-dimensional case and the widest – in the three-dimensional one. The values of the parameters used for plotting the graphs in Figs. 4–6 are the same as in Fig. 2.

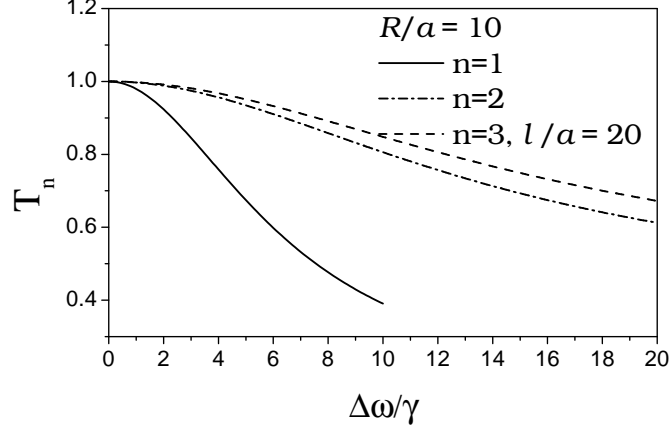


FIG. 6: Functions $T_n = \text{Re } S_R^{(n)}(\Delta\omega)/S_R^{(n)}(0)$, $n = 1, 2, 3$, for $R/a = 10$

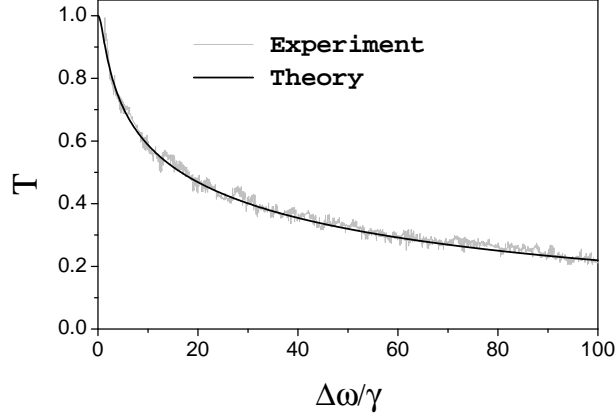


FIG. 7: Normalized transmission $T = \text{Re } S_R^{(3)}(\Delta\omega)/S_R^{(3)}(0)$ — comparison with experiment

V. COMPARISON WITH EXPERIMENT

Figure 7 shows the comparison of the results of numerical calculations with experimental data [13]. The calculations were performed for the dimensionless parameters

$$\begin{aligned}\hat{\tau}_a &= 3.39 \times 10^{-4}, & \hat{\tau}_r &= 1.69 \times 10^{-3}, \\ \tau_\nu &= 1.00 \times 10^{-4}, & \hat{\tau}_D &= 2.30 \times 10^{-3}, \\ \hat{v}_0 &= 2.95 \times 10^3, & \hat{D} &= 4.35 \times 10^2, \\ \hat{R} &= 5, & \hat{l} &= 5\end{aligned}$$

close to the experimental conditions. One can see that our theoretical results are in rather good agreement with those of experimental measurements.

It is worth noting that the experimental data presented in Fig. 7 also agree well with the theoretical calculation of the transmission spectrum obtained by averaging over atom trajectories. This testifies to the fact that the proposed model is also in good agreement with that based on the averaging over trajectories [13, 16], at least in the cases where these theories can be consistently compared. The proposed model has a wider range of applications, since the model with averaging over trajectories can be used only for the case of an infinite cell (at least in its present form).

VI. CONCLUSIONS

We have constructed a model for the description of the phenomenon of Ramsey diffusion-induced narrowing of the transmission spectrum of atoms in a buffer-gas cell for the case of weak fields in the strong-collision approximation. This model can be used for an arbitrary intensity distribution of laser beams in the direction normal to their propagation. The general theory is illustrated by calculations for the Gaussian intensity distribution.

The analytical expressions for transmission spectra obtained with the help of the effective diffusion equation qualitatively agree with experimental data and the results obtained by averaging over atom trajectories. The proposed model gives a possibility to investigate the shape of the transmission spectrum as a function of not only the intensity distribution in the plane of the laser beam but also the size of the buffer-gas cell. We have considered different geometric configurations (one-, two-, and three-dimensional). Comparing the spectra for one-, two-, and three-dimensional models, one can see that the line becomes wider with increase in the dimension.

The work is carried out in the framework of Projects F28.2/035 and RFFD/1-09-25.

-
- [1] G. Alzetta, A. Gozzini, L. Moi, and G. Orriols, *Nuovo Cimento B* **36**, 5 (1976).
 - [2] E. Arimondo and G. Orriols, *Lett. Nuovo Cimento* **17**, 333 (1976).
 - [3] H.R. Gray, R.W. Whitley, and C.R. Stroud, jr., *Opt. Lett.* **3**, 218 (1978).
 - [4] S.E. Harris, *Phys. Today* **50**, 36 (1997).
 - [5] L.V. Hau, S.E. Harris, Z. Dutton, and C.H. Behroozi, *Nature (London)* **397**, 594 (1999).

- [6] S. Knappe, R. Wynands, J. Kitching, H.G. Robinson, and L. Hollberg, J. Opt. Soc. Am. B **18**, 1545 (2001).
- [7] K. Bergmann, H. Theur, and B.W. Shore, Rev. Mod. Phys. **70**, 1003 (1998).
- [8] W.W. Quivers, jr., Phys. Rev. A **34**, 3822 (1986).
- [9] M. Erhard and H. Helm, Phys. Rev. A **63**, 043814 (2001).
- [10] E. Arimondo, Phys. Rev. A **54**, 2216 (1996).
- [11] A.S. Zibrov and A.B. Matsko, Phys. Rev. A **65**, 013814 (2001).
- [12] A.S. Zibrov, I. Novikova, and A.B. Matsko, Opt. Lett. **17**, 1311 (2001).
- [13] Y. Xiao, I. Novikova, D.F. Phillips, and R.L. Walsworth, Phys. Rev. Lett. **96**, 043601 (2006).
- [14] N.F. Ramsey, *Molecular Beams* (Clarendon Press, Oxford, 1956).
- [15] N.F. Ramsey, Rev. Mod. Phys. **62**, 541 (1990).
- [16] Y. Xiao, I. Novikova, D.F. Phillips, and R.L. Walsworth, Optics Express **16**, 14128 (2008).
- [17] S.G. Rautian and I.I. Sobelman, Usp. Fiz. Nauk **90**, 209 (1966).
- [18] V.A. Alekseev, T.L. Andreeva, and I.I. Sobelman, Zh. Eksp. Teor. Fiz. **62**, 614 (1972).
- [19] V.A. Alekseev, T.L. Andreeva, and I.I. Sobelman, Zh. Eksp. Teor. Fiz. **64**, 813 (1973).
- [20] S.G. Rautian, Sov. Phys. Uspekhi Usp. Fiz. Nauk **34**, 1008 (1991).
- [21] *Handbook of Mathematical Functions with Formulas, Graphs, and Mathematical Tables*, edited by M. Abramowitz and I.A. Stegun (Dover, New York, 1974).
- [22] P.M. Morse, H. Feshbach, *Methods of Theoretical Physics* (McGraw-Hill, New York, 1953).

Translated from Ukrainian by H.G. Kalyuzhna

[23] Notation: $\text{Ei}_1(x) = \int_x^\infty \frac{e^{-t}}{t} dt.$